Observation of Rydberg-Valence Mixing in High-Resolution Symmetry-Resolved Oxygen K-Edge Spectra of O_2

Akira Yagishita and Eiji Shigemasa
Photon Factory, National Laboratory for High Energy Physics, Oho, Tsukuba 305, Japan

Nobuhiro Kosugi
Institute for Molecular Science, Myodaiji, Okazaki 444, Japan
(Received 27 April 1993; revised manuscript received 5 November 1993)

High-resolution symmetry-resolved O K-edge spectra of O_2 have been obtained by collecting fragment ions emitted parallel ($\Delta\Lambda = 0$) and perpendicular ($\Delta\Lambda = +1$) to the electric vector of the incident light. In the $\Delta\Lambda = 0$ spectrum some unassigned peaks are found in the $1s$-$3p\sigma$ Rydberg state, converging to the $^4\Sigma^-$ ionized state, on the resonance feature around 541 eV. Comparison with *ab initio* potential energy curves indicates that the $1s$-$3p\sigma(^4\Sigma^-)$ Rydberg state is mixed with the $1s$-σ^* repulsive state with the same ion core ($^4\Sigma^-$) and the avoided curve crossing enhances vibrational excitations. The resonance feature around 539.5 eV is attributed to the $1s$-$\sigma^*(^2\Sigma^-)$ state arising from the exchange splitting in the $1s$-σ^* excitations.

PACS numbers: 33.70.–w, 33.80.Eh, 33.80.Gj, 33.90.+h

The Rydberg structures in the O K-edge spectrum of O_2 were veiled as a consequence of insufficient energy resolution or signal-to-noise ratio, even after advances in photoabsorption and electron energy-loss spectroscopies [1–3]. Very recently Rydberg structures of O_2 have been unveiled using high-resolution soft x-ray synchrotron radiation [4–6]; several Rydberg peaks are clearly observed on the broad resonance absorption that is split into two main features, B and C, as shown in Fig. 1. Differing from the closed-shell N_2 [7] and CO [8] molecules, however, the open-shell O_2 molecule shows unusual near-edge structures that make it difficult to give definite interpretation. There still are some serious controversies on the assignment of the near-edge structures in spite of improved resolution [1–6, 9–11].

In our previous work we concluded that the resonance features B and C arise in the exchange splitting in the $1s$-$2p\sigma^*(3\sigma_u)$ excited states, where the lower $1s$-$2p\sigma^*$ state is related to the $^2\Sigma^-$ ion core and the higher one to the $^4\Sigma^-$, and found that most of the fine structures on the σ^* resonances are due to Rydberg transitions converging to the two ionization thresholds, $^4\Sigma^-$ and $^2\Sigma^-$, and that the $p\sigma$-type Rydberg series show relatively intense structures [6]. Although we were aware that the $1s$-$3p\sigma$ and $4p\sigma$ Rydberg states with the $^4\Sigma^-$ ion core are observed near the higher $1s$-$2p\sigma^*$ excited state with the same ion core, we could not find experimental evidence of the Rydberg-valence mixing. In order to shed light on the conflicting arguments of the two resonance features B and C and the Rydberg-valence mixing, we have developed a new detection system which makes it possible to measure the symmetry-resolved spectra using much more highly monochromatic synchrotron radiation, and calculated *ab initio* configuration interaction (CI) potential energy curves for the $1s$ excited and ionized states of O_2.

Experiments were carried out using the 10-m grazing-incidence monochromator [12] installed at the soft x-ray undulator beam line [13] of the Photon Factory storage ring. Fragment photoions emerging from the interaction region, in which monochromatic synchrotron radiation and O_2 gas beams crossed, were detected by three channeltrons operated at a time. The channeltrons were set at 0°, 54.7° (magic angle), and 90° relative to the electric vector of the incident light. The acceptance angles of the orifices in front of the channeltrons were ±10°. To eliminate thermal molecular ions the positive voltage of 2 V was applied to the retardation electrodes which were made of a net of mesh and were located between the interaction region and the channeltrons. The channeltron set at 0° collects fragment ions emitted through the decay processes following the $\Delta\Lambda = 0$ (referred to Σ hereafter) photoexcitation and the channeltron at 90° collects frag-

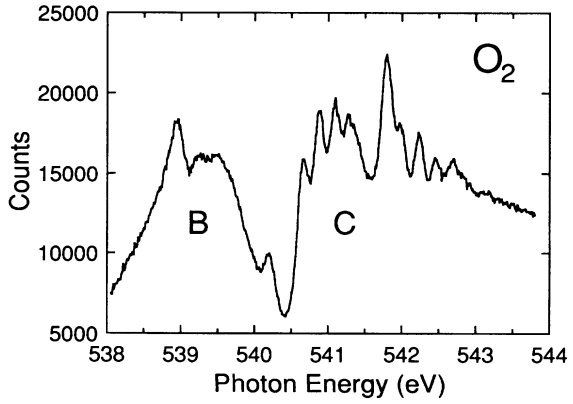

FIG. 1. A high-resolution total ion-yield spectrum at the O K-edge of O_2 with a resolving power of about 10 000. The Rydberg transitions are observed on the broad resonance features B and C.

ment ions emitted following the $\Delta\Lambda = +1$ (referred to $\prod$) one [6, 14–16].

We obtained diabatic potential energy curves by extended CI calculations to search for the Rydberg-valence mixing. The method is based on the first-order CI, allowing the single substitution to the virtual-orbital space from the full-valence space involving the O $1s$, $2s$, and $2p$ orbitals. In the CI calculations the Rydberg states are excluded. We have drawn diabatic potential energy curves for the Rydberg states by referring to the potential energy curves of the ionized states and the term values obtained in the previous work [6]. Primitive basis functions were taken from (73/7) contracted Gaussian-type functions of Huzinaga *et al.* [17]. They were augmented with one d polarization function ($\zeta_d = 1.154$). The contraction schemes were (4111111/31111/1*) and (721/511/1*) for the ionized and unionized oxygen atoms, respectively; in the former basis the innermost $2s$ exponent was changed to 2.003 92 from 10.195 52. In the core-hole states calculated the hole is kept localized. The calculations were performed by using the originally developed code GSCF3 [18, 19] on a MIPS RS3330 workstation.

Figure 2(a) shows the symmetry-resolved O K-edge spectra of O_2 measured with a resolving power of about 5000. The spectra obtained by the channeltrons at 0° (Σ) and 90° ($\prod$) were normalized so that their sum could coincide with the spectrum obtained by the channeltron at the magic angle, which corresponds to the total ion-yield spectrum. Figure 2(b) shows the blowup of the $\Delta\Lambda = 0$ ion-yield (Σ) spectrum with the peak assignments, and Fig. 2(c) shows the $\Delta\Lambda = +1$ ion-yield ($\prod$) spectrum. There are four candidates of dipole-allowed Rydberg series in the $\prod$ spectrum [Fig. 2(c)]: $np\pi$ and $nd\pi$ series converging to the $^4\Sigma^-$ core-ionized state, and $np'\pi$ and $nd'\pi$ series converging to the $^2\Sigma^-$ state. The exchange splitting in the Rydberg series is not so different from the splitting in the core-ionized states of $^4\Sigma^-$ and $^2\Sigma^-$ (1.1 eV), though the exchange splitting in the core-excited ($1s$-σ^*) state is completely different from that in the core-ionized states as predicted by our previous limited CI calculation (–2.75 eV [6]) and present extended CI calculation (–1.64 eV). Taking into account the term values and oscillator strengths for the Rydberg transitions [6], we have assigned peaks in the Σ and $\prod$ spectra as indicated in Figs. 2(b) and 2(c).

At the resonance feature B shown in the Σ spectrum [Fig. 2(b)] the $1s$-$3s\sigma(^4\Sigma^-)$ Rydberg state lies simply on the $1s$-$2p\sigma^*(^2\Sigma^-)$ state with no Rydberg-valence mixing, because the $1s$-$2p\sigma^*$ and $1s$-$3s\sigma$ states have different ion cores. The σ^* resonance has a rather broad structure due to the bound-free transition arising from a repulsive potential energy curve of the $1s$-$2p\sigma^*(^2\Sigma^-)$ excited state as shown in Fig. 3 and discussed by Kuiper and Dunlap [11]. Therefore, we could speculate that the asymmetric $1s$-$3s\sigma(^4\Sigma^-)$ peak shows a Fano line shape due to interaction between a discrete Rydberg state and

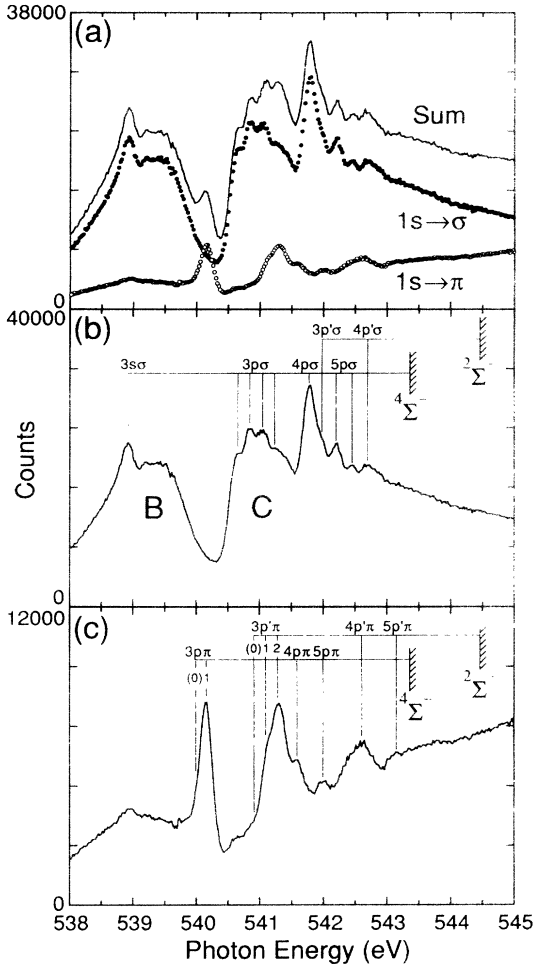

FIG. 2. High-resolution $\Delta\Lambda = 0$ (Σ) and $\Delta\Lambda = +1$ ($\prod$) ion-yield spectra ("symmetry-resolved" photoabsorption spectra) with a resolving power of about 5000: (a) symmetry-resolved spectra and their sum corresponding to the total ion-yield spectrum, (b) blowup of the Σ spectrum, and (c) blowup of the $\prod$ spectrum with the assignment of the Rydberg series. The vertical lines marked $^4\Sigma^-$ and $^2\Sigma^-$ indicate the energy positions of the ionization thresholds.

a dissociative continuum [20]. On the other hand, it is possible that the higher $1s$-$2p\sigma^*(^4\Sigma^-)$ state interacts with some $np\sigma(^4\Sigma^-)$ Rydberg states. In Fig. 2(b) the $np\sigma(^4\Sigma^-)$ Rydberg series ($n \geq 4$) and $np'\sigma(^2\Sigma^-)$ series ($n \geq 3$) show single peaks similarly to the $np\pi(^4\Sigma^-)$ and $np'\pi(^2\Sigma^-)$ Rydberg series, but the $3p\sigma(^4\Sigma^-)$ Rydberg transition cannot be assigned to a single peak. The potential energy curves shown in Fig. 3 clearly show that the $1s$-$2p\sigma^*(^4\Sigma^-)$ repulsive state strongly interacts with the $1s$-$3p\sigma(^4\Sigma^-)$ Rydberg state in the Franck-Condon region and that the transition to a new bound state (upper state) produced through the avoided curve crossing can have several vibrational excitations. We believe that the $1s$-$3p\sigma(^4\Sigma^-)$ Rydberg excited state is

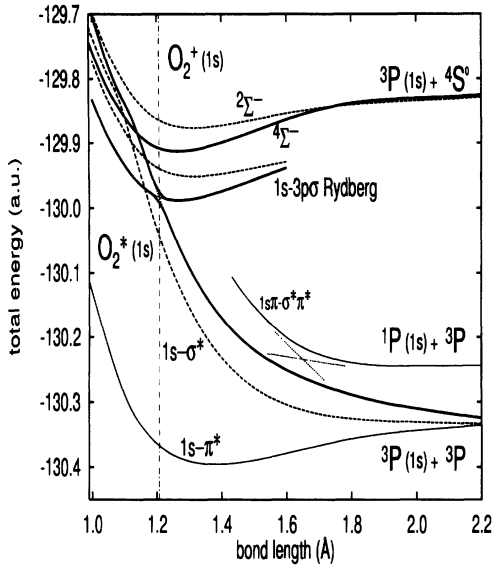

FIG. 3. Potential energy curves for O 1s excited and ionized states calculated with the first-order CI method. The solid and broken lines denote the potential energy curves of the states with the $^4\Sigma^-$ and $^2\Sigma^-$ ion cores, respectively. The equilibrium bond length of the ground state is 1.207 Å. The avoided curve crossing between the 1s-3$p\sigma$($^4\Sigma^-$) and 1s-σ^*($^4\Sigma^-$) states, namely Rydberg-valence mixing, is found in the Franck-Condon region, and causes vibrational enhancement in the transition to the upper state.

strongly perturbed by the 1s-2$p\sigma^*$($^4\Sigma^-$) excited state with a repulsive potential energy curve and shows unusual vibrational structures.

The present high-resolution symmetry-resolved spectrum shows that the 3$p\pi$($^4\Sigma^-$) and 3$p'\pi$($^2\Sigma^-$) Rydberg peaks are asymmetric, where the latter is broader in the low energy side than the former. This indicates that the $^4\Sigma^-$ and $^2\Sigma^-$ core-ionized states have different equilibrium geometries from the $^3\Sigma_g^-$ ground state (R = 1.207 Å). This agrees with the equilibrium bond lengths obtained with the *ab initio* SCF calculations by Ågren *et al.* [21] (1.276 Å for $^4\Sigma^-$, 1.331 Å for $^2\Sigma^-$) and the ones with the present *ab initio* CI calculations (1.264 Å for $^4\Sigma^-$, 1.314 Å for $^2\Sigma^-$). As was discussed in the high-resolution O 1s XPS spectrum of O_2 by Larsson *et al.* [22], the bond length of 1.26–1.28 Å gives the peak maximum of the 1s-3$p\pi$($^4\Sigma^-$) Rydberg excitation lying between the v = 0 and v = 1 vibrational levels and the bond length of 1.31–1.33 Å gives the peak maximum of the 1s-3$p'\pi$($^2\Sigma^-$) one at the v = 2 level.

Wurth *et al.* [9], Ruckman *et al.* [10], and Kuiper and Dunlap [11] calculated the exchange splitting by assuming that the lower 1s-2$p\sigma^*$ state has an electron configuration [1$s\downarrow$ $\pi^*\uparrow\uparrow$ $\sigma^*\uparrow$] and the higher one has [1$s\uparrow$ $\pi^*\uparrow\uparrow$ $\sigma^*\downarrow$]. We presented more appropriate description of the spin couplings in the $^3\Sigma^-$ 1s-2$p\sigma^*$ excited states by mixing at least configurations such as [1$s\uparrow$ $\pi^*\uparrow\downarrow$ $\sigma^*\uparrow$] with the above configurations [6]. Our previous limited CI treatment of the open-shell spin couplings predicts a large exchange splitting of 2.75 eV due to large exchange integrals between the 1s and σ^* electrons and between the σ^* and π^* electrons [6], whereas the treatment by Wurth *et al.* [9], Ruckman *et al.* [10], and Kuiper and Dunlap [11] ignores the exchange interaction between the 1s and σ^* electrons and underestimates the exchange splitting (1.2 eV [9], 0.4 eV [10,11]). In the present extended CI calculation the exchange splitting is decreased to 1.64 eV due to mixing with doubly excited configurations as suggested by Kuiper and Dunlap [11], but is still so large as to assign the features B and C (splitting $\simeq$1.75 eV) to the exchange splitting. Based on the solid-phase spectrum of O_2, Ruckman *et al.* [10] and Kuiper and Dunlap [11] assigned the two 1s-2$p\sigma^*$ excitations to only the feature B and found a crossing between the 1s-2$p\sigma^*$($^2\Sigma^-$) and 1s-2$p\sigma^*$($^4\Sigma^-$) states in the Franck-Condon region. As shown in Fig. 3 such a crossing does occur at about 1.1 Å and does not contribute in the Franck-Condon region. They interpreted the feature C' in the solid-phase spectrum as the intermolecular charge-transfer band [10] and as the ionization thresholds [11] and the feature C in the gas-phase spectrum as the Rydberg transitions [10], based on complete absence of Rydberg states in the solid-phase spectrum. In the spectra of the physisorbed and multilayer O_2 molecules recently reported [11,23–25], the polarization dependence of the feature B' indicates clearly the σ symmetry but that of the feature C' does not so clearly indicate the σ symmetry, and in the spectra of the physisorbed O_2/Ag(110) [24] we cannot identify the feature C'. It is partly because in the physisorbed and multilayer O_2 the ionization thresholds decrease in energy and the continuum contributes largely to the feature C' and partly because in the physisorbed and multilayer O_2 some π-symmetry Rydberg states are incompletely quenched or are alive as exciton states.

Kuiper and Dunlap [11] found atomic Auger lines from the ^3P atomic O 1s-2p excited state in the Auger spectrum by tuning the photon energy at the feature B' of solid O_2 and indicated rapid dissociation of O_2 following the excitation to the 1s-2$p\sigma^*$ excited states with repulsive potential curves. The exchange splitting estimated by them is about 1 eV for the ^3P and ^1P atomic O 1s-2p excited states [(1s)^1(2s)^2(2p)^5]. Schaphorst *et al.* [26] found atomic Auger lines more clearly in the gas-phase spectrum taken at the feature B (540.0 eV) and found only the atomic Auger lines from the ^3P atomic O 1s-2p excited state [27]. Their findings mean that the 1s-2$p\sigma^*$ state which contributes to the feature B has a dissociative channel to the ^3P atomic O 1s-2p excited state. The exchange splittings calculated in the present work are 5.06 eV for the ^4P and ^2P atomic O 1s ionized states [(1s)^1(2s)^2(2p)^4] and 3.01 eV for the ^3P and ^1P atomic O 1s-2p excited states [(1s)^1(2s)^2(2p)^5], which are in good

agreement with the experimental data (4.87 eV [27] and 2.9 eV [26]), respectively. The potential energy curve in Fig. 3 clearly indicates that the $1s\text{-}2p\sigma^*(^2\Sigma^-)$ state related to the feature B is directly dissociated to the ^3P atomic O $1s\text{-}2p$ excited state with no curve crossing, in agreement with the observation by Schaphorst *et al.* [26]. Furthermore, they could find no atomic Auger lines from the ^3P or ^1P atomic O $1s\text{-}2p$ excited state by tuning the photon energy at the feature C. Their finding means that the molecular Auger decay takes place before the dissociation in the $1s\text{-}2p\sigma^*(^4\Sigma^-)$ repulsive state related to the feature C, where it should be noticed that the $1s\text{-}2p\sigma^*(^4\Sigma^-)$ state is correlated to the ^3P atomic O $1s\text{-}2p$ excited state through a large avoided crossing with the $1s\pi\text{-}\sigma^*\pi^*$ doubly excited state as shown in Fig. 3. This result supports our finding of the Rydberg-valence mixing at the feature C; the excited state has longer lifetime in the bound state produced by the Rydberg mixing in the $1s\text{-}2p\sigma^*(^4\Sigma^-)$ repulsive state as shown in Fig. 3.

Very recently, Neeb *et al.* [28] have assigned the two $1s\text{-}2p\sigma^*$ excitations to only the feature B and obtained the value of 0.6 eV as an experimental exchange splitting in the gas phase. Their interpretation is based on the difference between the resonance Auger spectra, or de-excitation electron spectra, following the core-to-valence and core-to-Rydberg transitions. However, they did not take into account two important features in the O_2 inner-shell excitations at all, that is, Rydberg-valence mixing and atomic Auger decay. Therefore, their conclusion is much less convincing than the present one.

We wish to thank Professor A. P. Hitchcock, Dr. D. Arvanitis, and Dr. T. Yokoyama for their valuable discussion on the interpretation of the near-edge features, Dr. P. Kuiper and Dr. M. O. Krause for informing of their recent results prior to publication, and Professor T. Sasaki and Professor T. Matsushita for their extensive interest in the present work. This research is supported in part by Grant-in-Aid for Scientific Research on Priority Area "Theory of Chemical Reactions" from the Ministry of Education, Science, and Culture.

[1] G. R. Wight and C. E. Brion, J. Electron Spectrosc. **4**, 313 (1974).
[2] A. P. Hitchcock and C. E. Brion, J. Electron Spectrosc. **18**, 1 (1980).
[3] V. N. Akimov, A. S. Vinogradov, and T. M. Zimkina, Opt. Spectrosc. (U.S.S.R.) **53**, 63 (1982).
[4] Y. Ma, C. T. Chen, G. Meigs, K. Randall, and F. Sette, Phys. Rev. A **44**, 1848 (1991).
[5] K. J. Randall, J. Feldhaus, W. Erlebach, A. M. Bradshaw, W. Eberhardt, Z. Xu, Y. Ma, and P. D. Johnson, Rev. Sci. Instrum. **63**, 1367 (1992).
[6] N. Kosugi, E. Shigemasa, and Y. Yagishita, Chem. Phys. Lett. **190**, 481 (1992).
[7] C. T. Chen, Y. Ma, and F. Sette, Phys. Rev. A **40**, 6737 (1989).
[8] M. Domke, C. Xue, A. Puschmann, T. Mandel, E. Hudson, D. A. Shirley, and G. Kaindl, Chem. Phys. Lett. **173**, 122 (1990).
[9] W. Wurth, J. Stöhr, P. Feulner, X. Pan, K. R. Bauchspiess, Y. Baba, E. Hudel, G. Rocker, and D. Menzel, Phys. Rev. Lett. **65**, 2426 (1990).
[10] M. W. Ruckman, J. Chen, S. L. Qiu, P. Kuiper, M. Strongin, and B. I. Dunlap, Phys. Rev. Lett. **67**, 2533 (1991).
[11] P. Kuiper and B. I. Dunlap, J. Chem. Phys. **100**, 4087 (1994).
[12] A. Yagishita, S. Masui, T. Toyoshima, H. Maezawa, and E. Shigemasa, Rev. Sci. Instrum. **63**, 1351 (1992).
[13] A. Yagishita and E. Shigemasa, Rev. Sci. Instrum. **63**, 1383 (1992).
[14] E. Shigemasa, K. Ueda, Y. Sato, T. Sasaki, and A. Yagishita, Phys. Rev. A **45**, 2915 (1992).
[15] A. Yagishita, E. Shigemasa, J. Adachi, and N. Kosugi, in Proceedings of the 10th International Conference on Vacuum Ultraviolet Physics (to be published).
[16] E. Shigemasa, T. Hayaishi, T. Sasaki, and A. Yagishita, Phys. Rev. A **47**, 1824 (1993).
[17] S. Huzinaga, J. Andzelm, M. Kłobukowski, E. Radzio-Andzelm, Y. Sakai, and H. Tatewaki, *Gaussian Basis Sets for Molecular Calculations* (Elsevier, Amsterdam, 1984).
[18] N. Kosugi and H. Kuroda, Chem. Phys. Lett. **74**, 490 (1980).
[19] N. Kosugi, Theor. Chim. Acta **72**, 149 (1987).
[20] P. Kuiper (private communication).
[21] H. Ågren, L. Selander, J. Nordgren, C. Nordling, and K. Siegbahn, Chem. Phys. **37**, 161 (1979).
[22] M. Larsson, P. Baltzer, S. Svensson, B. Wannberg, N. Mårtensson, A. Naves de Brito, N. Correia, M. P. Keane, M. Carlsson-Göthe, and L. Karlsson, J. Phys. B **23**, 1175 (1990).
[23] R. J. Guest, A. Nilsson, O. Björneholm, B. Hernnäs, A. Sandell, R. E. Palmer, and N. Mårtensson, Surf. Sci. **269/270**, 432 (1992).
[24] R. J. Guest, B. Hernnäs, P. Bennich, O. Björneholm, A. Nilsson, R. E. Palmer, and N. Mårtensson, Surf. Sci. **278**, 239 (1992).
[25] D. Arvanitis, T. Yokoyama, T. Lederer, G. Comelli, M. Tischer, and K. Baberschke, Jpn. J. Appl. Phys. **S32-2**, 371 (1993).
[26] S. J. Schaphorst, C. D. Caldwell, M. O. Krause, and J. Jiménez-Mier (to be published).
[27] C. D. Caldwell and M. O. Krause, Phys. Rev. A **47**, R759 (1993).
[28] M. Neeb, J.-E. Rubensson, M. Biermann, and W. Eberhardt, Phys. Rev. Lett. **71**, 3091 (1993).